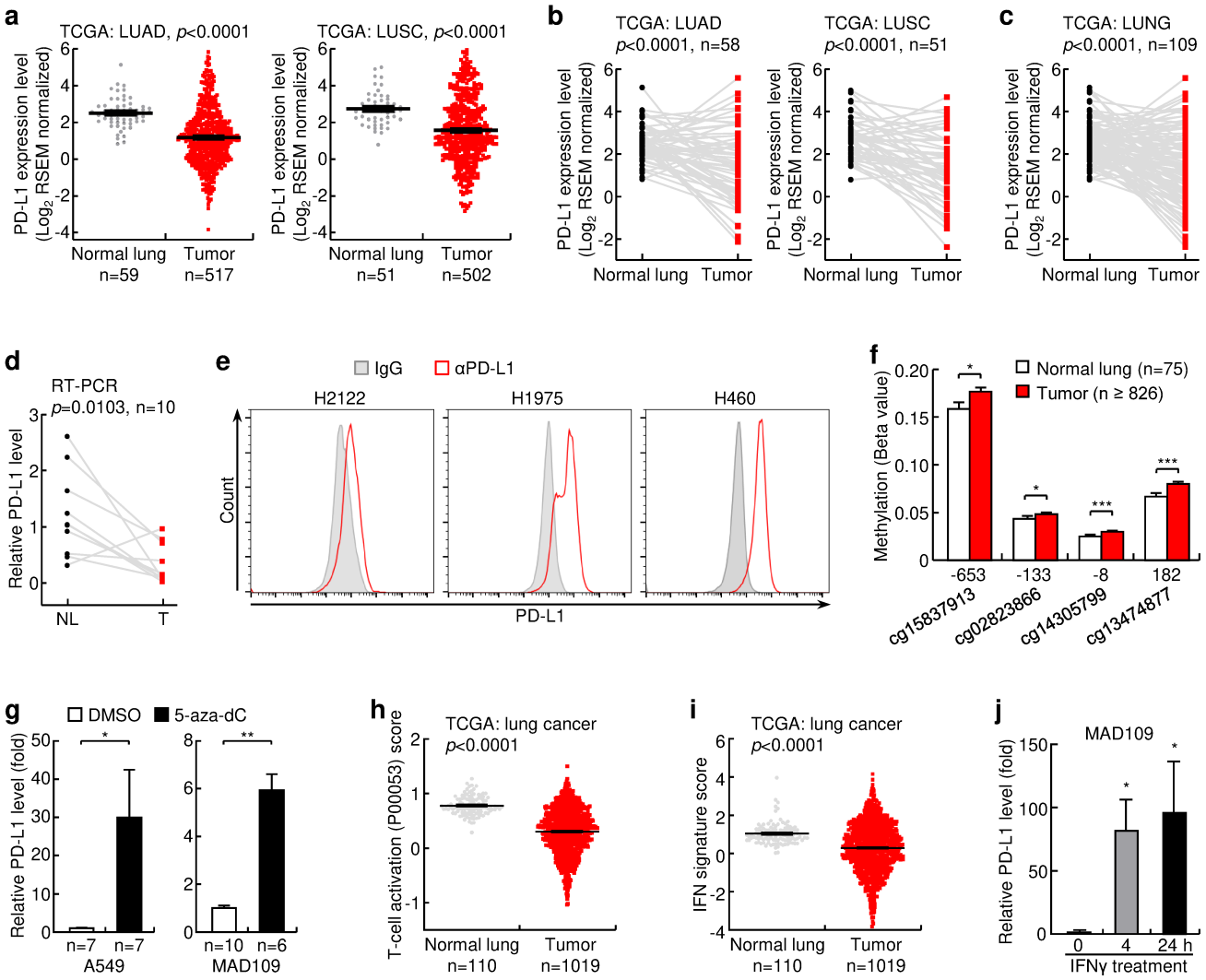

Supplementary Fig. S1 PD-L1 is downregulated in the majority of human lung cancers and PD-L1 downregulation in lung cancer involves its promoter methylation and inflammation repression. **a** TCGA data showing PD-L1 downregulation in human lung adenocarcinoma (LUAD) and squamous cell carcinoma (LUSC), two most common types of lung cancer that account for about 40% and 30% of all lung cancers, respectively. Grey dots and red dots stand for normal lung tissues and lung tumor tissues, respectively. **b** and **c** TCGA data showing PD-L1 downregulation in human lung cancers using paired lung tumor tissues and adjacent normal tissues from the same patients. **d** qPCR analysis showing PD-L1 downregulation in human lung cancers using paired lung tumor tissues (T) and adjacent normal lung tissues (NL) from the same patients. Student's *t* test (two tailed, paired) was performed in (**b**-**d**). **e** FACS analysis showing low PD-L1 expression on H2122 but high on H1975 or H460 human lung cancer cell lines. **f** TCGA data showing increased CpG methylation of the *pd-l1* promoter in human lung cancer. The position of CpG nucleotides relative to the *pd-l1* transcription initiation site (+1) and their probes are indicated at the bottom. **g** qPCR showing demethylating agent 5-aza-dC (0.5 μM) induction of PD-L1 expression in A549 (5 days) and MAD109 (3 days) lung cancer cells. **h** and **i** TCGA data showing decreased T-cell activation and IFN signature gene expression in human lung cancer. **j** qPCR showing IFNγ (20 ng/ml) induction of PD-L1 expression in MAD109 lung cancer cells (n = 5 for 0 and 4 h, n = 4 for 24 h).

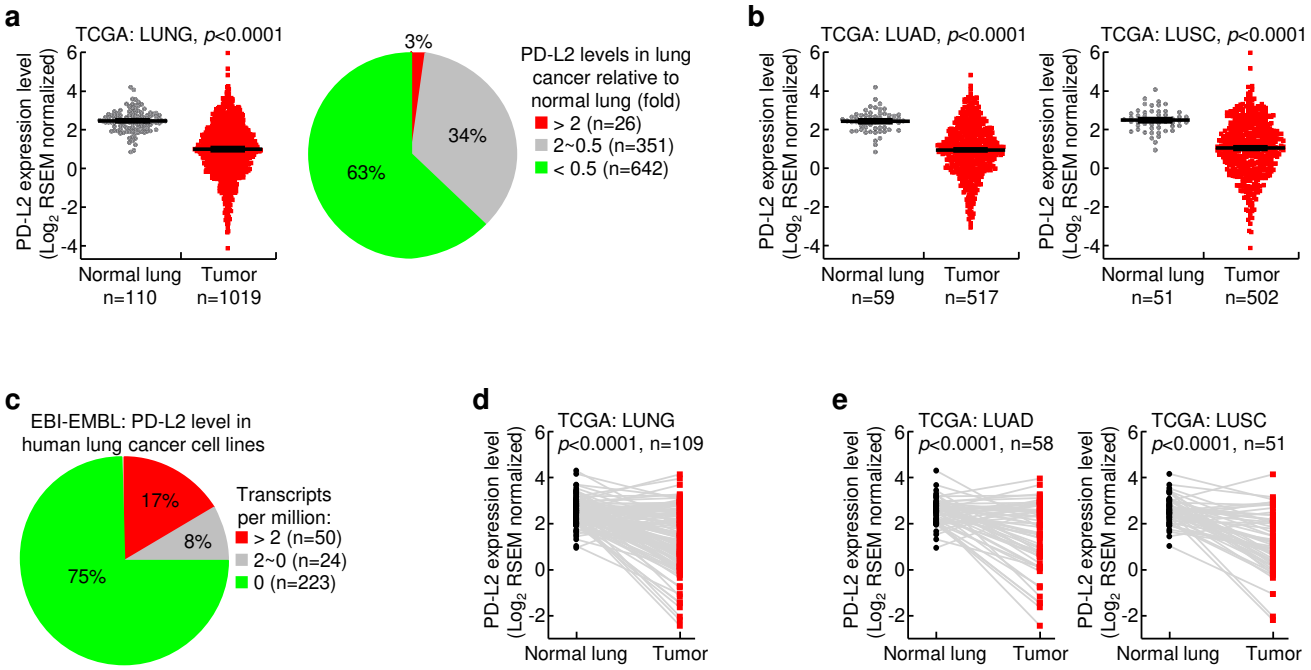

Supplementary Fig. S2 PD-L2 is downregulated in the majority of human lung cancers. **a** TCGA data showing PD-L2 downregulation in human lung cancer. Left: grey dots and red dots stand for normal lung tissues and lung cancer tissues, respectively. Right: PD-L2 expression profile in lung cancer tissues. Sample numbers are indicated. **b** TCGA data showing PD-L2 downregulation in human LUAD and LUSC subtypes. **c** EMBL-EBI data showing PD-L2 downregulation in human lung cancer cell lines. **d** and **e** TCGA data showing PD-L1 downregulation in human lung cancers using paired lung cancer tissues and adjacent normal tissues from the same patients.

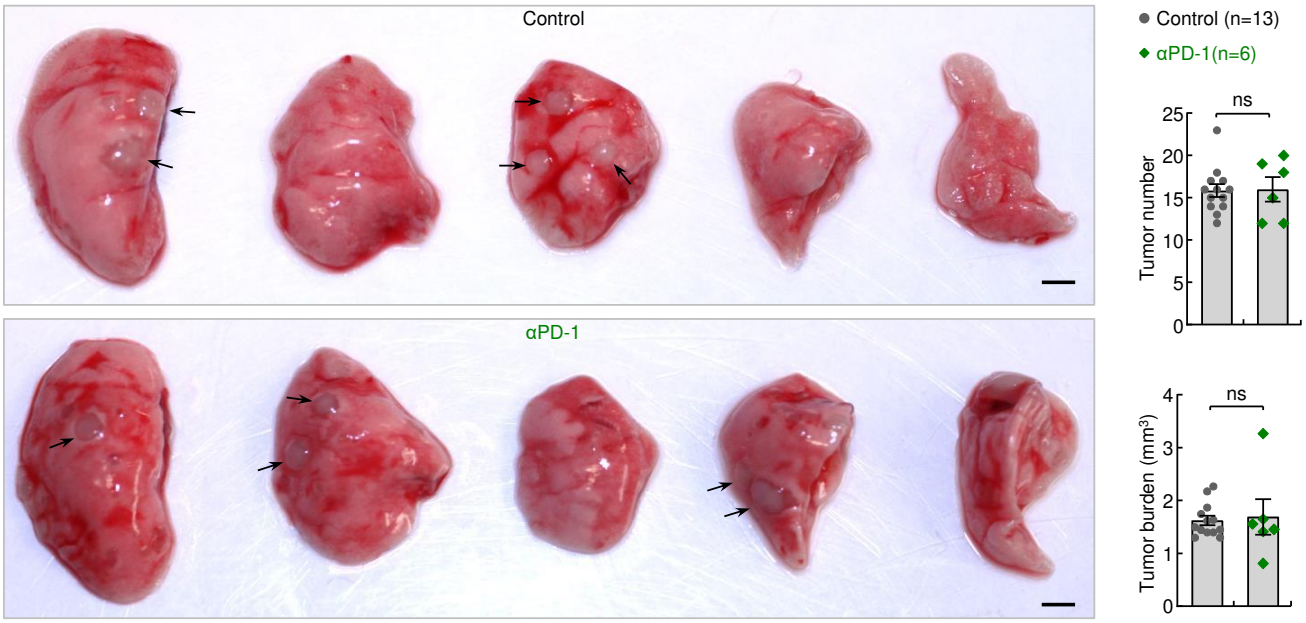

Supplementary Fig. S3 Mouse lung cancers induced by urethane are largely resistant to PD-1 blockade therapy. Scale bar, 1 mm. Student's t test (two tailed, unpaired) was performed.

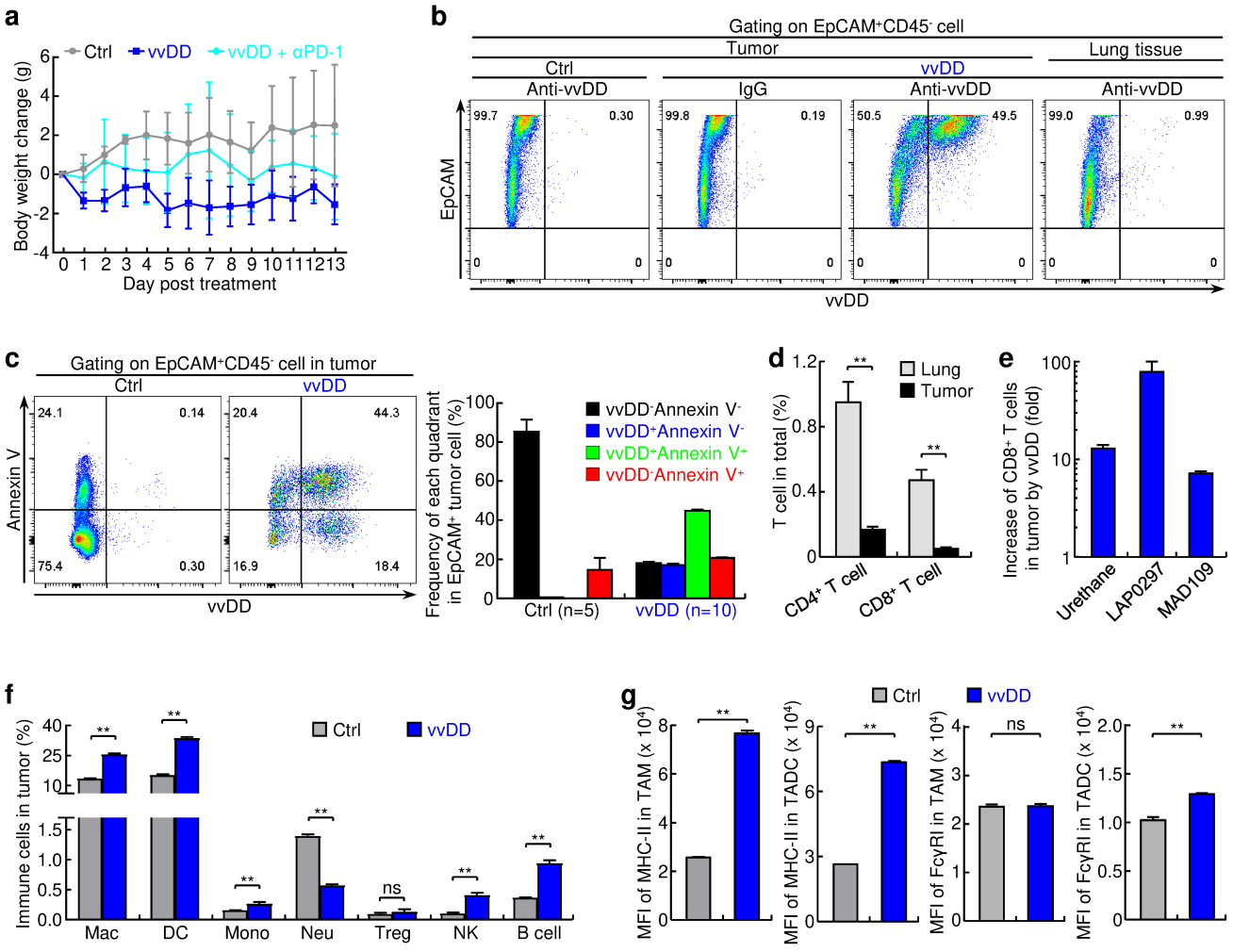

Supplementary Fig. S4 vvDD treatment induces tumor cell apoptosis and anti-tumor immune changes in lung cancer without causing significant side effects. **a** Mouse weight monitoring showing no significant effect on body weight by vvDD alone or together with PD-1 antibody in urethane model (n = 3). **b** FACS assays showing tumor cell-specificity of vvDD after its systemic delivery in urethane model. **c** FACS assays showing increased apoptosis in vvDD$^+$ tumor cells in urethane model. Mice were sacrificed 2 days post systemic delivery of vvDD by tail vein intravenous injection in (**b**, **c**). Note, this apoptosis detection is based on annexin V binding to phosphatidylserine (PtdSer), a marker of apoptosis that is also a ligand of TIM-3, on the outer leaflet of the cellular membrane, and therefore can also be used to detect this TIM-3 ligand. **d** FACS assays showing decreased tumor-infiltrating lymphocytes (TILs) compared to normal lung tissues in urethane model (n = 6). **e** FACS assays showing vvDD treatment increased tumor-infiltrating CD8$^+$ T cell in urethane-induced lung tumors (n = 3), syngeneic MAD109 tumors (n = 8) and syngeneic LAP0297 tumors (n = 5). **f** FACS assays showing the effects of vvDD treatment on immune cell populations within lung tumors in urethane model (n = 3). **g** FACS assays showing vvDD induction of MHCII and FcγRI expression on tumor-associated macrophages (TAM) and dendritic cells (TADC) in urethane model (n = 3).

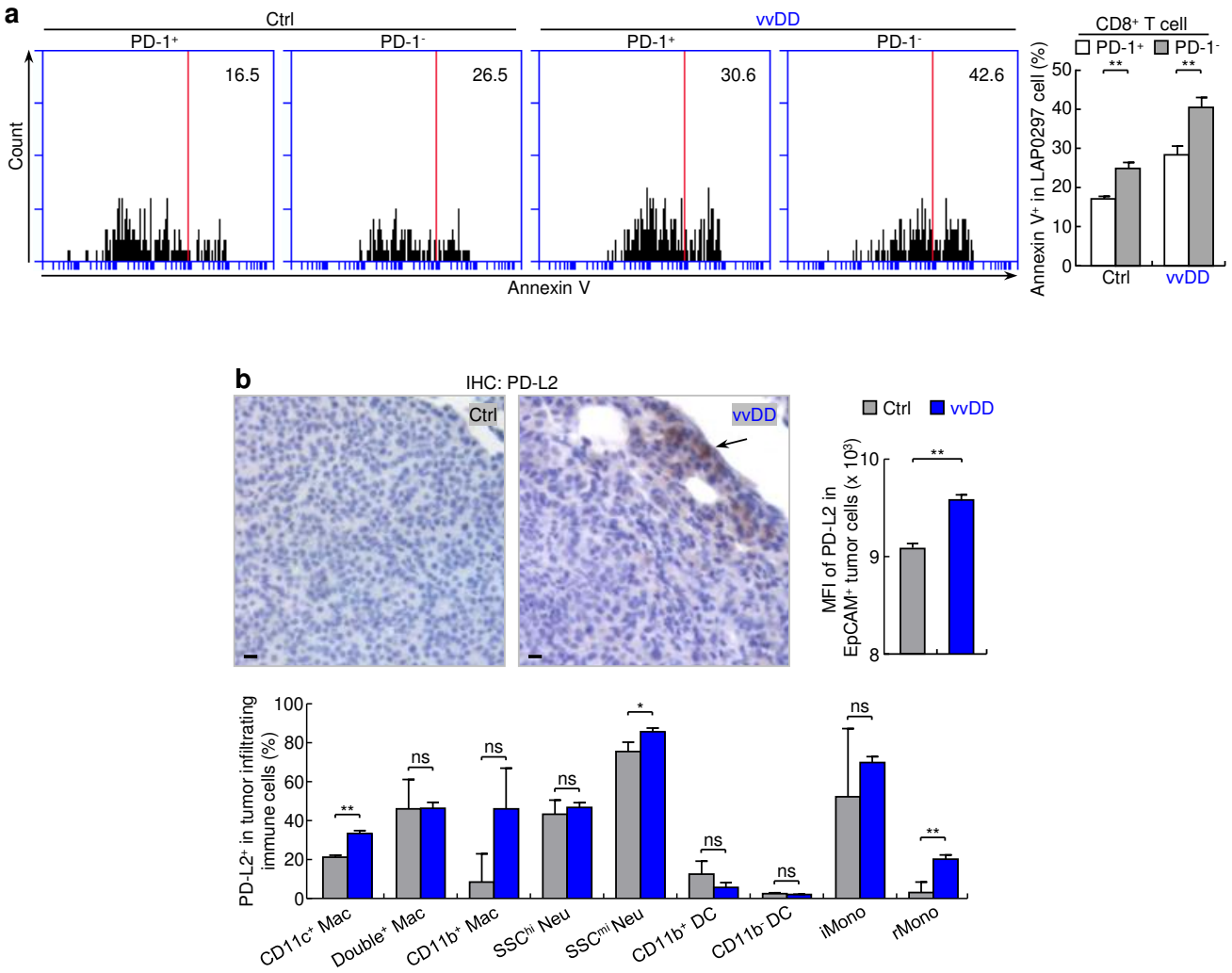

Supplementary Fig. S5 Treatment with vvDD increases tumor killing ability of tumor-infiltrating CD8⁺ T cells and induces PD-L2 expression on tumor cells and tumor-associated immune cells. **a** Co-culture assays showing a better antitumor cytotoxic ability of PD-1⁻CD8⁺ T cells compared to PD-1⁺CD8⁺ T cells and vvDD increase of this antitumor cytotoxicity in both PD-1⁻CD8⁺ T cells and PD-1⁺CD8⁺ T cells (n = 3). CD45⁺CD3⁺CD8⁺ cells were sorted from s.c. LAP0297 tumor and co-cultured with LAP0297 cells at a ratio of 1:1 (CD8⁺:LAP0297). Four hours later, the apoptosis in tumor cells were detected by FACS. **b** IHC and FACS assays showing increased PD-L2 expression on tumor cells and tumor-associated immune cells by vvDD treatment in urethane model (n = 3; Mac: macrophage; Neu: neutrophil; SSC: side scatter; hi: high; mi: middle; DC: dendritic cell; iMono: inflammatory monocyte; rMono: resident monocyte). Scale bar: 20 μm.

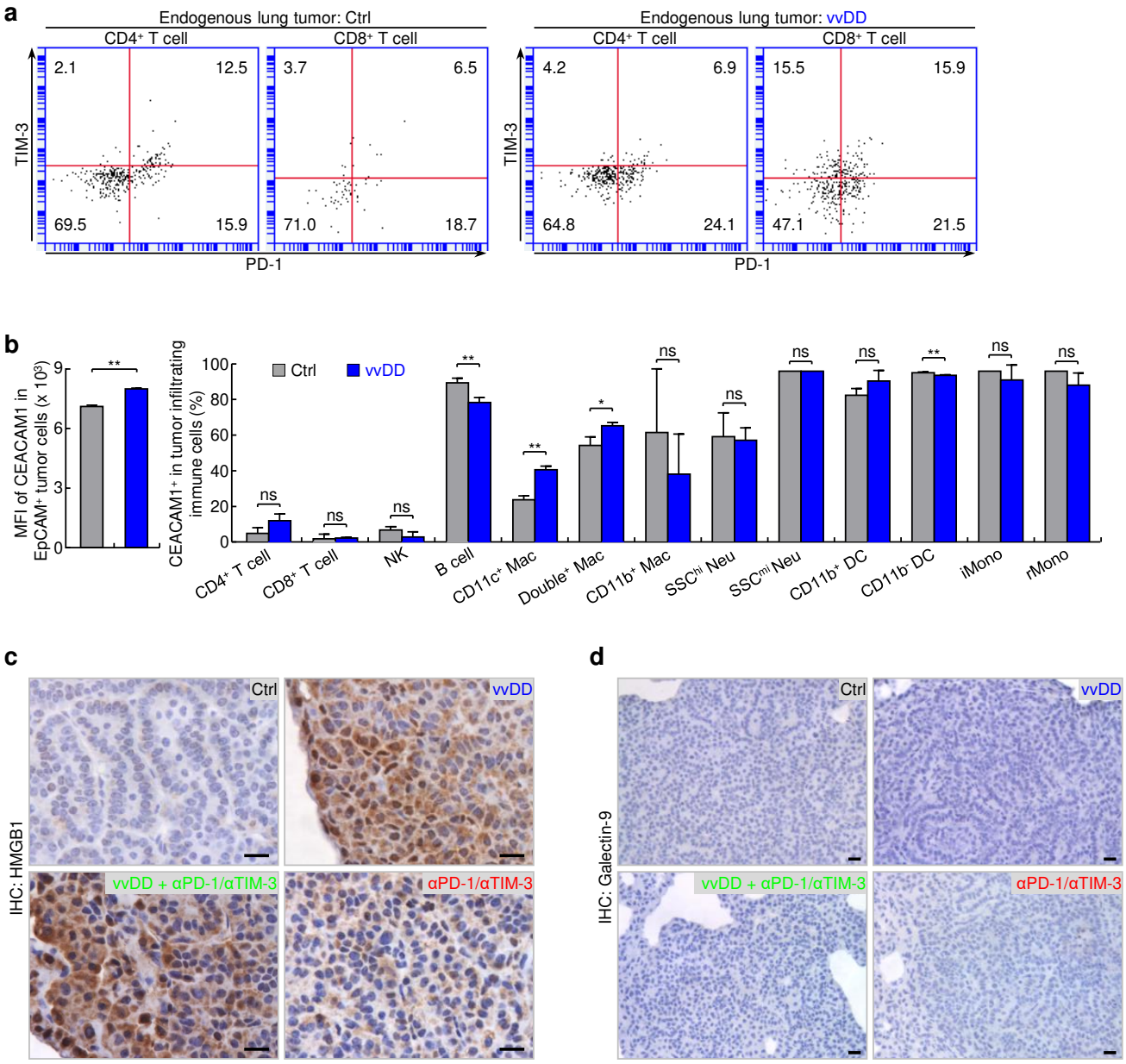

Supplementary Fig. S6 vvDD treatment alone or together with PD-1/TIM-3 antibody increases TIM-3 expression on CD8⁺ T cells and TIM-3 ligands expression in urethane-induced lung tumors. **a** FACS assays showing vvDD induction of PD-1 and TIM-3 expression on tumor-infiltrating CD8⁺ T cells. **b** FACS assays showing the effects of vvDD treatment on TIM-3 ligand CEACAM1 in urethane-induced lung tumors and tumor-associated immune cells (n = 3; NK: natural killer cell; Mac: macrophage; Neu: neutrophil; SSC: side scatter; hi: high; mi: middle; DC: dendritic cell; iMono: inflammatory monocyte; rMono: resident Monocyte). **c-d** IHC assays showing the effects of vvDD and/or αPD-1/αTIM-3 treatment on TIM-3 ligands HMGB1 (**c**) and Galectin-9 (**d**) in urethane-induced lung tumors. Scale bar: 20 μm.

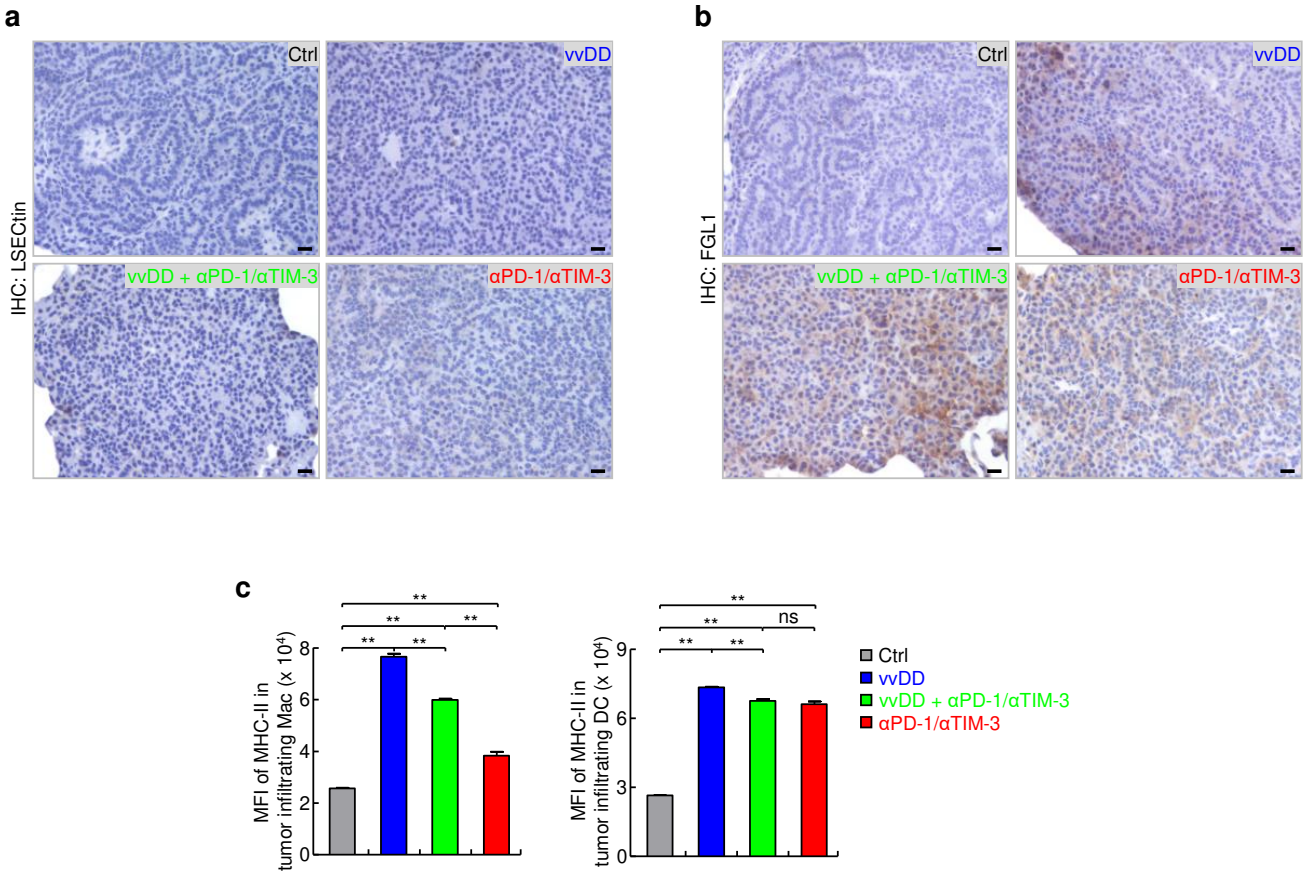

Supplementary Fig. S7 Effects of vvDD and/or αPD-1/αTIM-3 treatment on LAG-3 ligands expression in urethane-induced lung tumors. **a-b** IHC assays showing the effects of vvDD and/or αPD-1/αTIM-3 treatment on the expression of LAG-3 ligands LSECtin (**a**) and FGL1 (**b**) in urethane-induced lung tumors. Scale bar: 20 μm. **c** FACS assays showing induction of MHC-II expression on tumor-infiltrating macrophages and dendritic cells by vvDD and/or αPD-1/αTIM-3 treatment (n = 3).

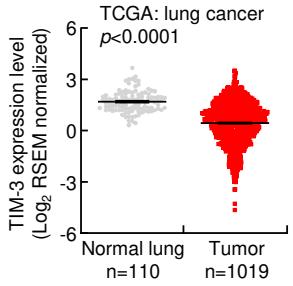

Supplementary Fig. S8 TCGA data showing decreased TIM-3 expression in human lung cancer.

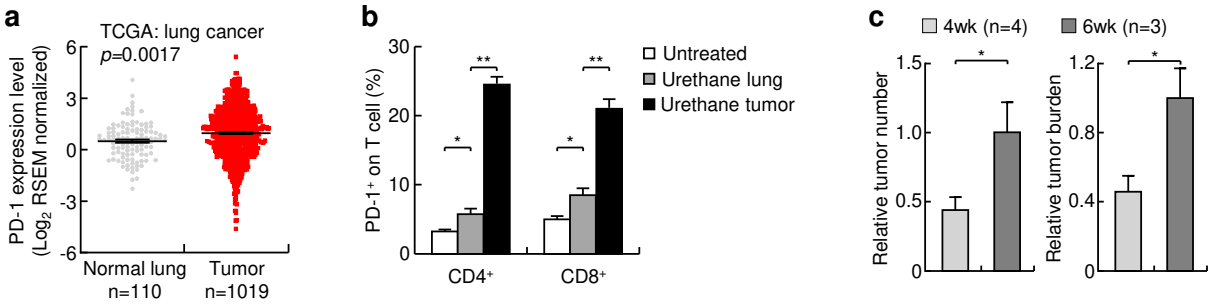

Supplementary Fig. S9 Increased PD-1 expression in human lung cancer and additional characterization of urethane-induced murine lung tumor model. **a** TCGA data showing increased PD-1 expression in human lung cancer. **b** FACS assays showing induction of PD-1 expression on $CD4^+$ T cells and $CD8^+$ T cells by urethane in normal mouse lungs and lung tumors (n = 3). **c** The relative tumor number and burden at the initiation of the treatment compared to the endpoint of the studies in urethane model.

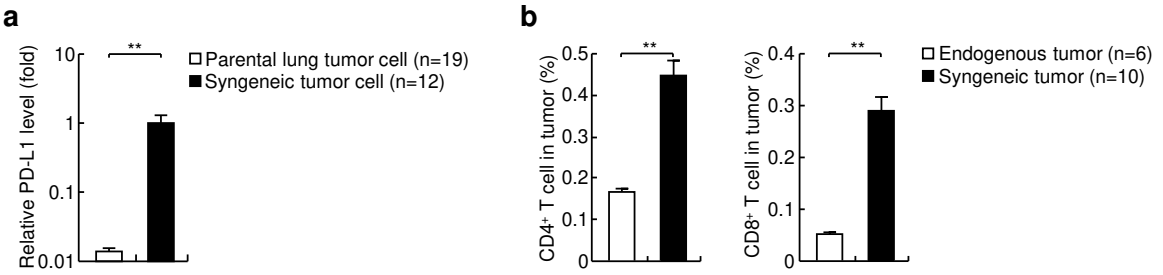

Supplementary Fig. S10 Syngeneic lung tumors show high PD-L1 expression and T-cell infiltration. **a** qPCR analysis showing PD-L1 re-expression in syngeneic MAD109 lung tumors. **b** FACS assays showing significantly more tumor-infiltrating $CD4^+$ and $CD8^+$ T cells in syngeneic MAD109 lung tumors in comparison to endogenous lung tumor.

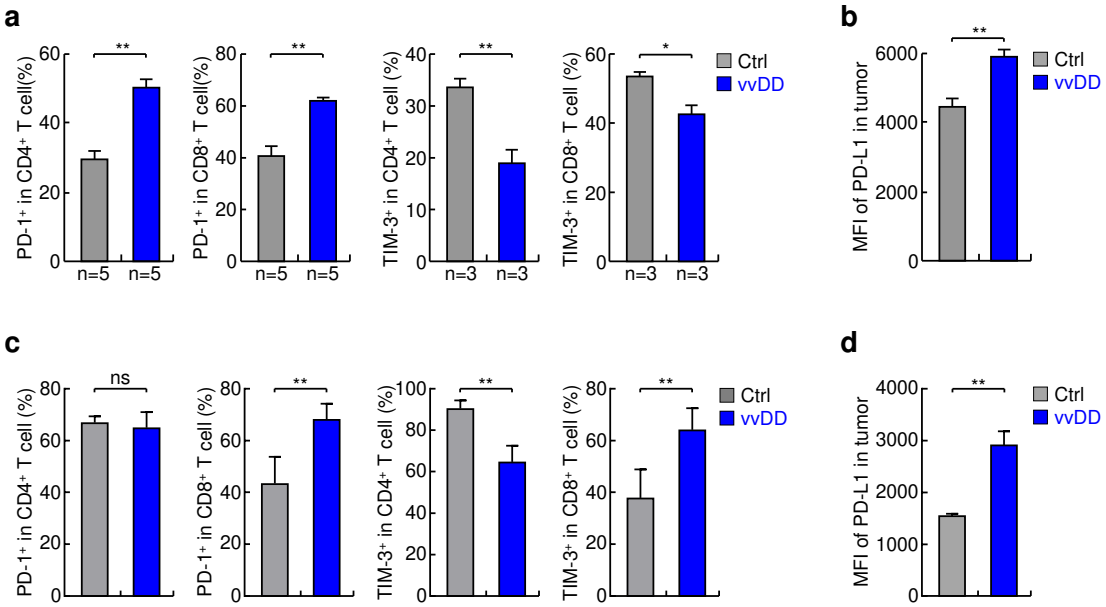

Supplementary Fig. S11 vvDD shows complex effects on tumor-infiltrating CD4⁺ and CD8⁺ T cell PD-1 and TIM-3 expression in different syngeneic models. **a** FACS assays showing increased PD-1 but decreased TIM-3 expression on tumor-infiltrating CD4⁺ and CD8⁺ T cells by vvDD treatment in syngeneic MAD109 tumors. **b** FACS assays showing increased PD-L1 expression on syngeneic MAD109 tumors by vvDD treatment (n = 5). **c** FACS assays showing increased PD-1 and TIM-3 expression on tumor-infiltrating CD8⁺ T cells but decreased TIM-3 expression on tumor-infiltrating CD4⁺ T cells by vvDD treatment in syngeneic LAP0297 tumors (n = 5). **d** FACS assays showing increased PD-L1 expression on syngeneic LAP0297 tumors by vvDD treatment (n = 5).

Table S1. Antibodies Used

Antibody	Company	Cat. No.	Dose	Usage
Anti-Cleaved Caspase 3	Cell Signaling Technology, Danvers, MA, USA	9661	1 : 200	IHC
Anti-PD-L1 (human)	Cell Signaling Technology, Danvers, MA, USA	13684	1 : 200	IHC
Anti-PD-L1 (mouse)	Cell Signaling Technology, Danvers, MA, USA	64988	1 : 200	IHC
Anti-PD-L2	Abcam, Cambridge, MA, USA	ab21107	1 : 50	IHC
Anti-Galectin 9	Biolegend, San Diego, CA, USA	137901	1 : 50	IHC
Anti-LSECtin	Abcam, Cambridge, MA, USA	ab181196	1 : 200	IHC
Anti-HMGB1	Invitrogen, Carlsbad, CA, USA	PA1-16926	1 : 200	IHC
Anti-FGL1	Invitrogen, Carlsbad, CA, USA	PA5-30030	1 : 200	IHC
Goat anti-rat IgG Biotinylated	Vector Laboratories, Burlingame, CA, USA	BA9401	1 : 100	IHC
Goat anti-rabbit IgG Biotinylated	Dako, Carpinteria, CA, USA	E0432	1 : 200	IHC
Anti-CD16/CD32	eBioscience, San Diego, CA, USA	14-0161-85	1.0 µl per sample	FACS
Anti-CD45 Alexa Fluor 700	Biolegend, San Diego, CA, USA	103128	0.5 µl per sample	FACS
Anti-CD45 FITC	Biolegend, San Diego, CA, USA	103107	0.5 µl per sample	FACS
Anti-PD-L1 SB780	eBioscience, San Diego, CA, USA	78-5982-82	0.3 µl per sample	FACS
Anti-PD-L2 PerCP/Cy5.5	Biolegend, San Diego, CA, USA	107218	1.25 µl per sample	FACS
Anti-CEACAM1 FITC	Biolegend, San Diego, CA, USA	134518	0.5 µl per sample	FACS
Anti-EpCAM PE	eBioscience, San Diego, CA, USA	12-5791-82	0.625 µl per sample	FACS
Anti-EpCAM BV421	Biolegend, San Diego, CA, USA	118225	1.25 µl per sample	FACS
Anti-Annexin V APC	eBioscience, San Diego, CA, USA	17-8007-74	5 µl per sample	FACS
PI	eBioscience, San Diego, CA, USA	00-6990-42	5 µl per sample	FACS
Anti-CD3 PE	eBioscience, San Diego, CA, USA	12-0031-83	2.5 µl per sample	FACS
Anti-CD3e APC780	eBioscience, San Diego, CA, USA	47-0031-82	5 µl per sample	FACS
Anti-CD4 APC780	eBioscience, San Diego, CA, USA	47-0042-82	0.625 µl per sample	FACS
Anti-CD4 PE	eBioscience, San Diego, CA, USA	12-0041-83	0.625 µl per sample	FACS
Anti-CD4 PE-Cy7	eBioscience, San Diego, CA, USA	25-0042-82	1.25 µl per sample	FACS
Anti-CD8a APC	eBioscience, San Diego, CA, USA	17-0081-83	0.625 µl per sample	FACS
Anti-IFNγ FITC	eBioscience, San Diego, CA, USA	11-7311-82	1 µl per sample	FACS
Anti-GranzB FITC	eBioscience, San Diego, CA, USA	11-8898-82	0.25 µl per sample	FACS
Anti-CD69 FITC	eBioscience, San Diego, CA, USA	11-0691-85	1 µl per sample	FACS
Anti-CD44 PE-Cy7	eBioscience, San Diego, CA, USA	25-0441-81	0.625 µl per sample	FACS
Anti-PD-1 FITC	eBioscience, San Diego, CA, USA	11-9985-82	2 µl per sample	FACS
Anti-TIM-3 PE	eBioscience, San Diego, CA, USA	12-5871-81	0.3 µl per sample	FACS
Anti-LAG-3 FITC	eBioscience, San Diego, CA, USA	11-2231-82	2 µl per sample	FACS
Anti-CD11b PE	eBioscience, San Diego, CA, USA	12-0112-82	0.625 µl per sample	FACS
Anti-CD11c APC780	eBioscience, San Diego, CA, USA	47-0114-82	2.5 µl per sample	FACS
Anti-Ly6C BV650	Biolegend, San Diego, CA, USA	128049	1.25 µl per sample	FACS
Anti-Ly6G BV510	Biolegend, San Diego, CA, USA	127633	2.5 µl per sample	FACS

Anti-MerTK SB436	eBioscience, San Diego, CA, USA	62-5751-82	5 µl per sample	FACS
Anti-CD64 PE-Cy7	Biolegend, San Diego, CA, USA	139314	2.5 µl per sample	FACS
Anti-MHCII APC	eBioscience, San Diego, CA, USA	17-5321-82	0.15 µl per sample	FACS
Anti-NKp46 BV421	Biolegend, San Diego, CA, USA	137612	2.5 µl per sample	FACS
Anti-B220 BV510	Biolegend, San Diego, CA, USA	103248	2.5 µl per sample	FACS
Anti-CD25 PE	eBioscience, San Diego, CA, USA	12-0251-81	0.625 µl per sample	FACS
Anti-Foxp3 FITC	eBioscience, San Diego, CA, USA	11-5773-82	2 µl per sample	FACS
Anti-PD-1	BioXcell, West Lebanon, NH, USA	BE0273	200 µg/mouse/time	*in vivo* blockade
Anti-TIM-3	BioXcell, West Lebanon, NH, USA	BE0115	100 µg/mouse/time	*in vivo* blockade

Table S2. Primers Used

Gene	Species	Accession number	Forward (5' to 3')	Reverse (5' to 3')	Usage
gapdh	human	NM_002046.3	CCGAGCCACATCGCTCAGACAC	GTGACCAGGCGCCCAATACGAC	RT-PCR
cd274 (pd-l1)	human	NM_014143.3	TGGCATTTGCTGAACGCATTT	AGTGCAGCCAGGTCTAATTGT	RT-PCR
gapdh	mouse	NM_008084.2	AGTGCCAGCCTCGTCCCGTA	CAGGCGCCCAATACGGCCAA	RT-PCR
cd274 (pd-l1)	mouse	NM_021893.3	CCTGCTGTCACTTGCTACGG	CACTAACGCAAGCAGGTCCA	RT-PCR